NASA Technical Paper 2154

May 1983

Regression Analysis of Traction Characteristics of Two Traction Fluids

Stuart H. Loewenthal
and Douglas A. Rohn

NASA

25th Anniversary
1958-1983

NASA
Technical
Paper
2154

1983

Regression Analysis of Traction Characteristics of Two Traction Fluids

Stuart H. Loewenthal
and Douglas A. Rohn
Lewis Research Center
Cleveland, Ohio

NASA
National Aeronautics
and Space Administration

**Scientific and Technical
Information Branch**

Summary

A multivariable regression analysis was performed on traction data for two modern traction fluids, Santotrac 50 and TDF-88, over a wide range of operating conditions. For these tests maximum contact pressures ranged from 1.0 to 1.9 GPa; rolling speeds from 10 to 80 m/sec; oil inlet temperature from 27° to 73° C; contact ellipse ratios from 1 to 5; and spin angles from 0 to 30°. A total of 187 experimental traction curves for the Santotrac 50 and 147 traction curves for the TDF-88 fluid were analyzed. An eight-term correlation equation to predict the maximum traction coefficient μ, and a six-term correlation equation to predict the initial slope m of the traction curve were developed. Both μ and m must be known at the appropriate operating condition before a traction contact performance analysis, of the Johnson and Tevaarwerk type, for example, can be conducted. A performance analysis can be used to determine the traction, creep, spin torque, and contact power loss associated with a given traction contact. A simplified slope correction was developed to correct the slope correlation for size effect considering the compliance of the disks. The correlation equations developed were also used to study the effects of different operating conditions on the traction performance of each traction fluid.

The correlation equations fit the data reasonably well over the range of operating conditions. Both traction fluids exhibited a loss in traction with increases in spin, but the losses with the TDF-88 fluid were not as severe as those with Santotrac 50. Overall, both fluids exhibited similar performance, showing an increase in traction with contact pressure up to about 2.0 GPa, and a reduction in traction with higher surface speeds up to about 100 m/sec. The apparent stiffness of the traction contact, that is, film-disk combination, increases with contact pressure and decreases with speed.

Introduction

The traction characteristics of a lubricant are of great importance to the performance of many machine elements, such as bearings, gears, and traction drives. The effective traction coefficient occurring in the contact dictates the amount of slip in ball bearings, the skew in roller bearings, and the creep rate across a traction-drive contact. The product of the traction force and slip rate is also a direct measure of the load-dependent power loss of a rolling-element contact.

For traction drives the traction coefficient is the single most important parameter in determining its life, size, and performance. The fatigue life of a traction-drive contact has been theoretically shown to be proportional to the cube of the coefficient of traction for a given size and a constant torque level (ref. 1). It was also shown that the size of the traction drive is inversely proportional to the coefficient of traction to the 0.36 power.

The traction coefficient not only dictates the amount of traction that can be imposed across a traction contact without slip, but also determines the degree of creep and hence power loss that will be developed. In this regard, several theoretical investigations predict the performance of a traction-drive contact using the rheological characteristics of the lubricant as it passes through the elastohydrodynamic (EHD) contact (refs. 2 to 7). Contact pressure, temperature, shear rates, and lubricant composition all play important roles in determining whether the lubricant film exhibits viscous or elastic-solid behavior. It is now generally accepted (refs. 7 to 10) that, in most rolling-element contacts, the lubricant behaves elastically at small strain rates, that is, at low sliding speeds and that at higher sliding speeds the lubricant film exhibits highly nonlinear viscous behavior and tends to shear or "yield" like a plastic-solid. Thus, the lubricant's behavior in a traction contact can be modeled with reasonable accuracy as an elastic-plastic material having some characteristic shear modulus G and some limiting or critical yield stress τ_c (ref. 7). These two lubricant parameters, which vary with pressure, temperature, velocity, and contact geometry, must be determined under the appropriate operating conditions before traction contact performance calculations can be performed (refs. 11 and 12).

In a typical traction-drive contact, severe transient operating conditions are imposed on the lubricant. The lubricant is swept into the contact, exposed to contact pressures, which are 10 000 times atmospheric or greater, and returned to ambient conditions—all in a few milliseconds. Because of the difficulty of simulating the highly transient nature of an actual traction contact, fluid property data deduced from experimental traction curves (ref. 7) have given more satisfactory results in traction calculations than primary measurements from oscillatory shear viscosimeters or similar laboratory equipment. However, some progress has been made in resolving the computational differences in these two methods (ref. 13). In references 7, 11, and 12, Johnson and Tevaarwerk present a comprehensive traction-contact analysis which incorporates the lubricant's shear modulus and limiting shear stress in the form of several dimensionless parameters. These parameters can be written in terms of the maximum traction coefficient μ and the initial slope m from an experimental traction curve using the transformation methods described in references 7 and 11. Until recently, traction data for modern traction fluids over sufficiently broad operating conditions for design purposes has been relatively scarce (refs. 14 to 17). In reference 18 experimental traction data were obtained for two modern traction fluids over a range of speeds,

pressures, temperatures, contact ellipticity ratios, spin, and sideslip values encountered in traction drives. These data, although correlated against the major independent variables, were not presented in a form convenient for use in traction calculations. The objectives of the present investigation were to (1) perform a regression analysis on the data of reference 18 in order that the m and μ coefficients can be readily predicted at any intermediate operating condition, (2) develop a simplified slope correction that accounts for the compliance of the disk material, and (3) use the results of the regression analysis to study how these variables are affected by speed, pressure, temperature, ellipticity ratio, and spin.

Symbols

a	contact ellipse semiwidth transverse to direction of rolling, m
A_{11},A_{22}	Kalker coefficients in x and y direction, respectively
b	contact ellipse semiwidth in direction of rolling, m
C	lubricant contact parameter, $(3\pi/8)(m/\mu) \times \sqrt{k}$
$C_1, \ldots, C_8$	traction coefficient correlation coefficients
E	modulus of elasticity, Pa
E'	$=2/\left\{\left[(1-\nu_A^2)/E_A\right]+\left[(1-\nu_B^2)/E_B\right]\right\}$
F	surface traction force, N
G	elastic shear modulus, Pa
$\overline{G}$	apparent elastic shear modulus of contact system (film + disks), Pa
G_s	elastic shear modulus of disk material, Pa
g	Herztian contact size parameter, m
h_c	elastohydrodynamic central film thickness, m
$J_1, \ldots, J_7$	dimensionless traction parameters
$K_1, \ldots, K_7$	initial slope correlation parameters
k	contact ellipse ratio, a/b
m	initial slope of traction curve (film + disk)
m'	dry initial slope of traction curve (disk only)
N	normal load, N
R	regression coefficient
R_x,R_y	equivalent relative radii of curvature in x-and y-directions, respectively, m^{-1}
r	radius of curvature, m
$\hat{T}$	spin torque, N-m
T	temperature, °C
U	rolling surface velocity in x-direction, m/s
ΔU	longitudinal slip velocity, m/s
V	rolling surface velocity in y-direction, m/s
ΔV	sideslip velocity, m/s
α	lubricant pressure-viscosity coefficient, Pa^{-1}
ϵ	elliptical integral of the first kind
η_0	lubricant ambient absolute viscosity, poise (or $N{\cdot}S/m^2$)
μ	maximum traction coefficient of traction curve
μ_x,μ_y	traction coefficient in x- and y-directions, respectively
ξ	elliptical integral of the second kind
ρ	relative curvature sum, m^{-1}
σ_0	maximum contact pressure, Pa
τ_c	critical yield stress of film, Pa
ω_s	spin velocity, sec^{-1}
Superscripts:	
$'$	dry rolling body only
$*$	either second set of rollers or the rollers being analyzed
Subscripts:	
A,B	rolling-element bodies A and B
x,y	x (rolling) and y (normal to rolling) direction
f	lubricant film only

Performance Predictions

The distribution of local traction forces in the contact of an actual traction-drive can be rather complicated, as illustrated in figure 1 which shows the distribution of local traction vectors in the contact when longitudinal traction, misalinement, and spin are present. These traction forces will aline themselves with the local slip velocities. In a traction-drive contact, some combination of creep, misalinement, and spin is always present. To determine the performance of a traction-drive contact, the elemental traction forces must be integrated over the contact area.

In the 1960's and early 1970's numerous papers were presented on the prediction of traction in EHD contacts (refs. 19 to 21). About this time Poon (ref. 4) and Lingard (ref. 5) developed grid methods for shear stress integration to predict the available traction forces of a contact experiencing spin. Poon's method used the basic traction data from a twin-disk machine together with contact kinematics to predict the available traction. Lingard used a theoretical approach in which the EHD film exhibited a Newtonian viscous behavior at low shear

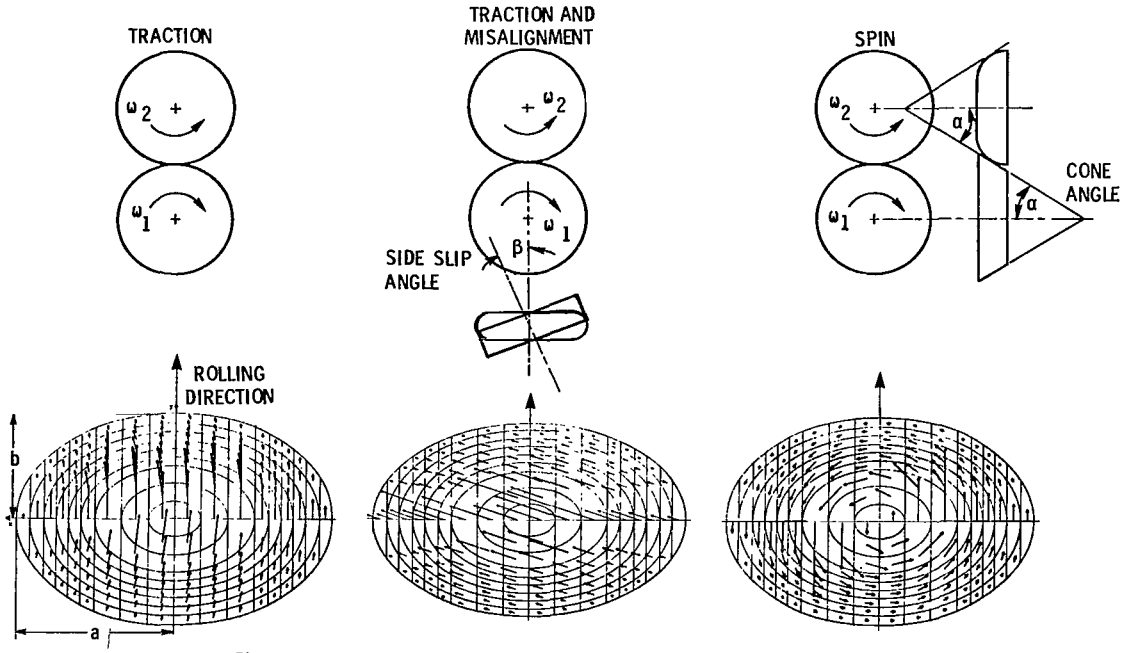

Figure 1. - Effect of misalinement and spin on contact traction force vectors.

rates until a critical limiting shear stress was reached. At this point the film yielded plastically with increasing shear rate. The most recent and perhaps most comprehensive traction-contact model is that proposed by Johnson and Tevaarwerk (refs. 7, 11, and 12). Their model covers the full range of viscous, elastic, and plastic behavior of the EHD film. This type of behavior depends on the Deborah number, a relative measure of elastic-to-inelastic response, and on the strain rate. At low pressures and speeds (low Deborah number), the film exhibits linear viscous behavior at low strain rates. It becomes increasingly more nonlinear with increasing strain rate. At higher pressures and speeds, more typical of traction-drive contacts, the response is linear and elastic at low rates of strain. At sufficiently high strain rates, the shear stress reaches some limiting value, and the film shears like a plastic solid, as in the case of some of the earlier traction analytical models (refs. 2 to 5).

Tevaarwerk presents graphical solutions developed from the Johnson and Tevaarwerk elastic-plastic traction model (refs. 11 and 12). These solutions are of practical value in the design and optimization of traction-drive contacts. By knowing m (related to shear modulus) and μ (related to limiting shear stress) from a zero-spin/zero-sideslip traction curve, the traction, creep, spin torque, and contact power loss can be found over a wide range of spin values and contact geometries.

In the Johnson and Tevaarwerk model, several dimensionless parameters were identified that best generalized the results of their analysis. These parameters can be written in terms of the shear modulus and limiting shear stress properties of the lubricant or in terms of the measured m and μ from a simple experimental traction curve (fig. 2). At this time it is more convenient and reliable to work with actual traction data rather than fundamental fluid property data. Fluid property data are usually generated under experimental conditions that are much different from those in a traction contact. For the Johnson and Tevaarwerk dimensionless groupings, slope and maximum traction coefficient data must be obtained from a zero-sideslip/zero-spin traction curve for the lubricant in question. These reference data must also be obtained at the same contact pressure, temperature, rolling speed, and for the same aspect ratio, area, and disk material as the contact to be analyzed. However, it is possible to use data obtained from tests where the ellipticity ratio and contact area are different if certain corrections are made to the slope, as will be shown. Traction data of two common traction fluids over a wide range of operating conditions appear later in this paper.

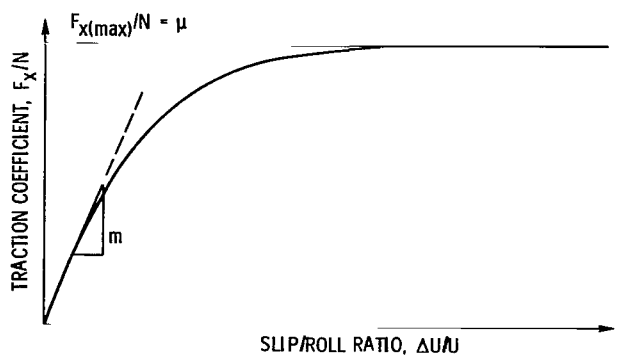

Figure 2. - Typical traction curve showing maximum traction coefficient μ and traction slope m.

With the Johnson and Tevaarwerk analysis, knowing just m and μ from a simple traction test leads to the prediction of the entire traction-creep curve under any combination of sideslip and spin. Also, the traction force transverse to the rolling direction and contact power losses can be readily determined.

The solutions to this analysis (refs. 11 and 12) are given in terms of the following dimensionless parameters:

Slip

$$J_1 = C\frac{\Delta U}{U} \tag{1}$$

Sideslip

$$J_2 = C\frac{\Delta V}{U} \tag{2}$$

Spin

$$J_3 = C\frac{\omega_s\sqrt{ab}}{U} \tag{3}$$

Traction

$$J_4 = \frac{\mu_x}{\mu} \tag{4}$$

Side traction

$$J_5 = \frac{\mu_y}{\mu} \tag{5}$$

Torque normal to the contact

$$J_6 = \frac{T}{\mu N\sqrt{ab}} \tag{6}$$

Total power loss

$$J_7 = J_4J_1 + J_5J_2 + J_6J_3 = \frac{C}{\mu NU}\left(F_x\,\Delta U + F_y\,\Delta V + \hat{T}\omega_s\right) \tag{7}$$

where C is lubricant contact parameter expressed as

$$C = \frac{3\pi}{8}\,\frac{m}{\mu}\,\sqrt{k} \tag{8}$$

The power loss term J_7 can be put in a more convenient form in terms of a loss factor L where

$$L = \frac{J_7}{J_4} = C\left(\frac{\text{power loss}}{\text{power input}}\right) \tag{9}$$

Thus, the ratio of power loss to power input may be determined from equation (9) by knowing the lubricant contact factor C and the loss factor L for the contact being analyzed.

Traction Fluid Data

To be able to apply the Johnson and Tevaarwerk analysis to the design of a traction contact, μ and m must be determined at the appropriate operating condition. Recently, experimental traction data of this type were obtained for Monsanto's Santotrac 50 and Sun Oil's TDF-88 over the range of operating conditions that might be encountered in a traction drive (ref. 18). The properties of these lubricants appear in table I. Approximately 191 and 152 separate traction tests were conducted with the Santotrac 50 and TDF-88 test fluids, respectively. Maximum contact pressures ranged from 1.0 to 1.9 GPa; rolling speeds from 10 to 80 m/sec; oil inlet temperatures from 27° to 73° C; contact ellipse ratios from 1 to 5; and spin angles from 0 to 30. A wide range of traction-versus-slip curves were obtained as illustrated in figure 3.

A twin-disk traction tester, is described in detail in references 9 and 18, was used to generate the traction data. Basically, the tester consists of a transversely crowned upper disk which is driven by a cylindrical lower disk, powered by a variable-speed electric motor. The

TABLE I. - TRACTION LUBRICANT PROPERTIES

Property	Lubricant	
	Santotrac 50	TDF-88
Kinematic viscosity, cm^2/sec (cS) at -		
311 K (100° F)	0.34 (34)	0.42 (42)
372 K (210° F)	0.056 (5.6)	0.054 (5.4)
Flash point, K (°F)	435 (325)	408 (275)
Fire point, K (°F)	447 (345)	428 (310)
Autoignition temperature, K (°F)	600 (620)	----------
Pour point, K (°F)	236 (-35)	236 (-35)
Specific heat at 311 K (100° F), J/kgK (Btu/lb °F)	2130 (0.51)	1895 (0.45)
Thermal conductivity at 311 K (100° F), J/m sec K (Btu hr ft °F)	0.10 (0.06)	0.11 (0.066)
Specific gravity at 311 K (100° F)	0.889	0.888

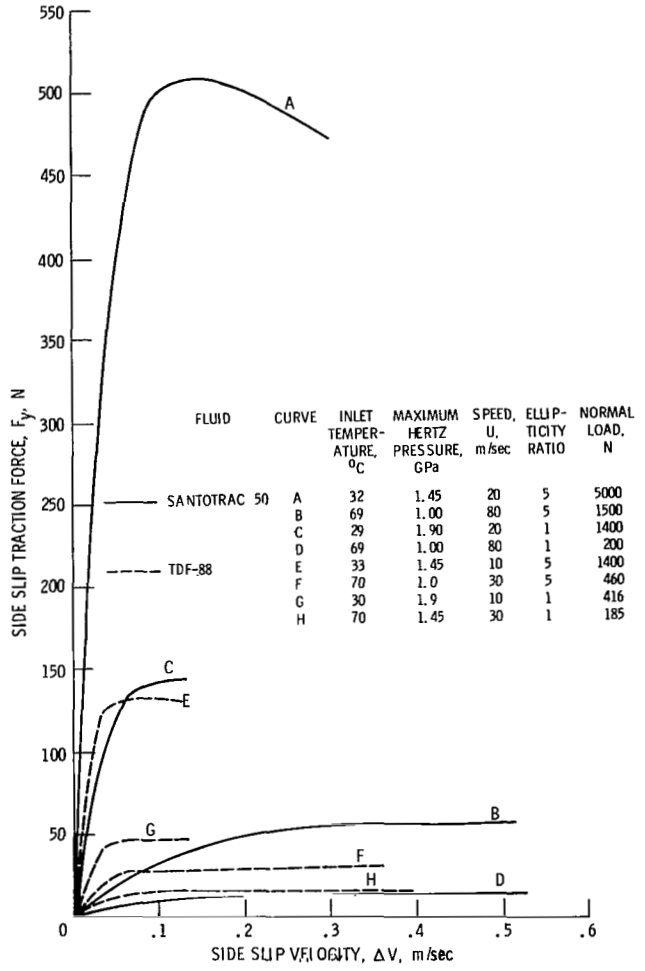

FLUID	CURVE	INLET TEMPERATURE, °C	MAXIMUM HERTZ PRESSURE, GPa	SPEED, U, m/sec	ELLIPTICITY RATIO	NORMAL LOAD, N
SANTOTRAC 50	A	32	1.45	20	5	5000
	B	69	1.00	80	5	1500
	C	29	1.90	20	1	1400
TDF-88	D	69	1.00	80	1	200
	E	33	1.45	10	5	1400
	F	70	1.0	30	5	460
	G	30	1.9	10	1	416
	H	70	1.45	30	1	185

Figure 3. - Range of typical side slip traction curves. (From ref. 68.)

upper disk is dead-weight loaded against the lower disk and is supported in a cradle that is free to pivot around a vertical axis to generate a sideslip velocity. The cradle can also tilt the upper disk as shown in figure 4 to generate angular spin velocity. The transverse radius of curvature of the upper disk can be varied to vary the contact ellipticity ratio.

Regression Analysis

To apply the Johnson and Tevaarwerk analysis to the design of traction-drive contacts, μ and m appearing in equations (1) to (9) must be determined at the proper operating speed, contact pressure, temperature, aspect ratio, and spin level for the lubricant in question. To accomplish this, a polynomial regression analysis was applied to the data of reference 18. The statistical techniques described in reference 22 were used.

Traction Coefficient

A total of 187 traction coefficient data points for the Santotrac 50 fluid and 147 data points for the TDF-88 fluid were analyzed. After successfully evaluating several forms of the regression equation, the following expression best represented the data with the fewest terms:

$$\mu = C_1 + C_2\sigma_0 + C_3\sigma_0^2 + C_4U + C_5U^2 + C_6T + C_7k + C_8\frac{\omega_s\sqrt{ab}}{U} \qquad (10)$$

The coefficients of this correlation equation for each of the test fluids are given in table II. The correlation's regression coefficient R, a measure of the fit of the regression equation, is equal to 0.884 for Santotrac 50 and 0.890 for TDF-88 fluid. (An R-value of 0 indicates no correlation; an R-value of 1.0 indicates a perfect correlation.) A comparison of predicted and measured μ data for the test fluids appears in figure 5. It should be remembered that the deviation between measured and predicted values is a function not only of the form of the correlation but also of the random error or scatter associated with the measurements. Thus, the value of R cannot attain 1.0 with experimental data, no matter how well the model fits (ref. 22).

Initial Slope

The m to be used in the Johnson and Tevaarwerk model is to be obtained from zero-spin traction curves. A

Figure 4. - Twin disk traction tester with upper disk tilted.

TABLE II. - COEFFICIENTS FOR MAXIMUM TRACTION COEFFICIENT CORRELATION EQUATION

Coefficient	Maximum traction coefficient, μ, for -	
	Santotrac 50	TDF-88
C_1	0.0726	0.0733
C_2	.0477	.0443
C_3	-.0102	-.0116
C_4	-6.92×10^{-4}	-7.36×10^{-4}
C_5	2.74×10^{-6}	2.38×10^{-6}
C_6	-2.13×10^{-4}	-9.08×10^{-5}
C_7	-3.41×10^{-4}	-1.88×10^{-3}
C_8	-1.22	-.433

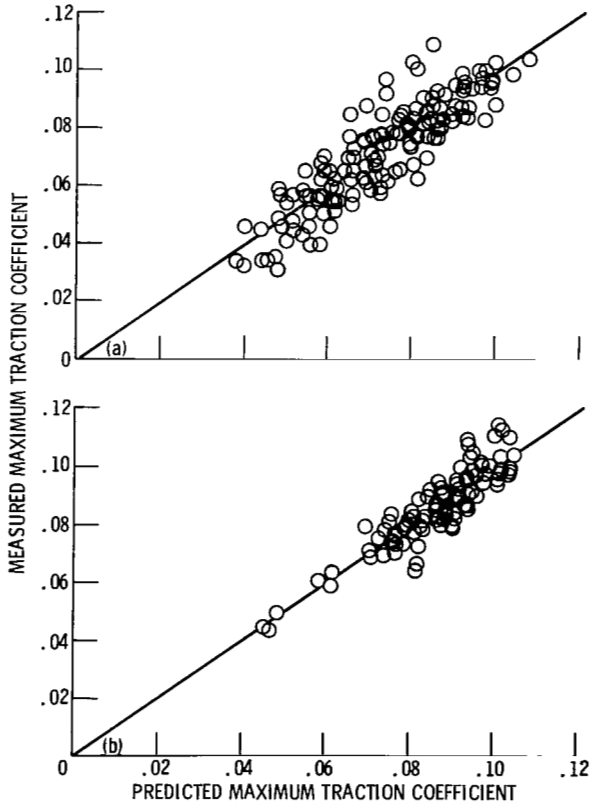

(a) For Santotrac 50.
(b) For TDF-88.

Figure 5. - Predicted and measured maximum traction coefficients.

regression analysis was performed on 73 and 101 slope data points for the Santotrac 50 and TDF-88 traction fluids, respectively. The regression model took the following form:

$$m = K_1 + K_2\sigma_0 + K_3 \ln(\sigma_0) + K_4 U + K_5 U^2 + K_6 T + K_7 k \quad (11)$$

Table III lists the coefficients for equation (11) for each of the test fluids. The R-values for the regression are 0.852 and 0.803 for Santotrac 50 and TDF-88, respectively. A comparison of predicted and measured m data appears in figure 6.

Slope Correction

The m of an experimental traction curve is a measure of the tangential stiffness or apparent shear modulus G of the lubricant film and metal surface combination. When the film is thin and stiff, as it is at low speeds and high pressures, the tangential deformation or compliance of the disk material is not negligible in comparison. Since the slope produced by the disks in dry contact (i.e., without a lubricant film) is independent of the disk size, while that produced by the film and disk system is not, a change in disk size will affect the measured slope of the film-disk system even if all of the remaining operating variables are kept the same. Thus to use slope data generated under identical operating conditions, but with disk of different size, an adjustment must be made. This adjustment can be made under the assumption that the elastic shear modulus of the film alone G_f will not be affected by changes in disk size under identical operating conditions. The approach to be taken is then to relate the shear modulus of the film to the measured slope of the film-disk system as follows.

TABLE III. - COEFFICIENTS FOR INITIAL SLOPE CORRELATION EQUATION

Coefficient	Initial slope, m, for -	
	Santotrac 50	TDF-88
K_1	101.4	51.3
K_2	-45.49	-6.53
K_3	69.44	17.20
K_4	.289	-.646
K_5	1.30×10^{-3}	4.99×10^{-3}
K_6	6.63×10^{-2}	.236
K_7	-2.99	-1.24

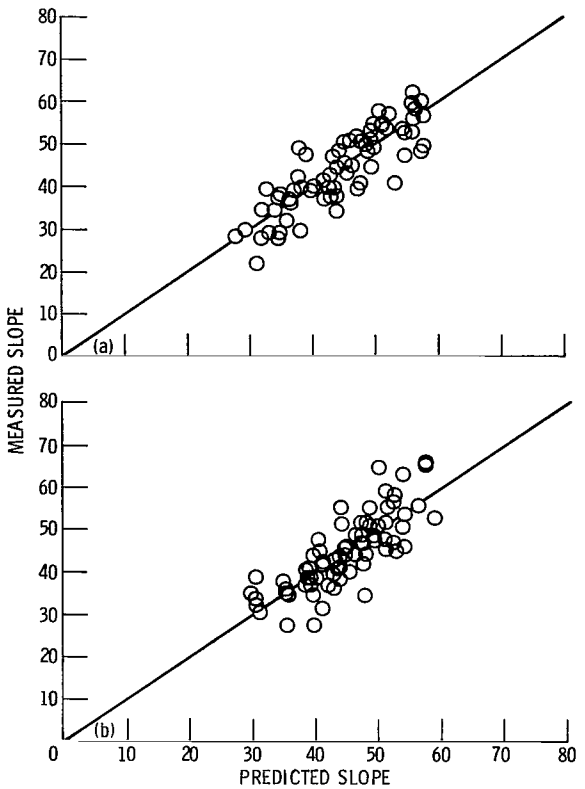

(a) For Santotrac 50.
(b) For TDF-88.

Figure 6. - Predicted and measured slopes.

Theory

The m is related to the apparent shear modulus of the contact system $\bar{G}$ by the expression (ref. 11):

$$m = \frac{4}{\pi} \frac{\bar{G}}{\sigma_0} \frac{b}{h_c} \tag{12}$$

Therefore, two systems having the same apparent shear modulus operating at the same pressure, temperature, velocity, and ellipticity ratio will have a different m, if the contact semiwidth b in the rolling direction or EHD central film thickness h_c are different. Thus, to use slope data generated experimentally with traction rollers of one size to predict the performance of a set of rollers running under the indentical operating conditions but of a different size, hence, different b and h_c, a slope correction factor must be applied. The correction factor is the ratio of the two initial slopes: m^*/m.

To develop a simple slope correction factor, the compliance of the disk material ($1/m'$) must be separated from the compliance of the contact system ($1/m$). In this way the compliance of the lubricant film ($1/m_f$) may be determined (ref. 23). As in the case of two springs in series, the compliance of the film and disk system is the summation of the compliance of each element as follows:

$$\frac{1}{m} = \frac{1}{m_f} + \frac{1}{m'} \tag{13}$$

where m is the slope of the film and disks together as normally measured, m_f is the slope produced by lubricant film alone, and m' is the slope produced by a dry rolling body.

In accordance with the Johnson and Tevaarwerk model (ref. 11), the lubricant is thought to behave elastically at small strain rates. It therefore follows that the shear modulus of the film G_f is proportional to the slope of the traction curve produced by the lubricant film alone. Thus, the apparent modulus of the contact system $\bar{G}$ can be corrected using equation (13) to approximately determine the modulus of the film alone as follows:

$$\bar{G}_f = \frac{m_f}{m} \bar{G} = \left(\frac{m'}{m' - m} \right) \bar{G} \tag{14}$$

The above compliance correction assumes that the fluid film behaves elastically over the entire contact, when in fact it will behave elastically only in the center of the contact where the Hertzian pressures are sufficiently high. A more detailed analysis (ref. 24) numerically integrates the tangential traction distribution throughout the elastic region of the contact and gives fluid shear moduli that are significantly higher than those given by equation (14). However, the interest here is to determine the *relative* effect that changes in contact area and EHD film thickness have on shear moduli or, more specifically, slope under the given operating conditions. It is therefore expected that on a relative basis the simplified correction adopted here will give acceptable results.

Using the assumption of reference 11 that, for slope measurements made with disks of different geometry but under identical pressure, speed, and temperature, the elastic shear modulus of the film with one set of disks G_f would be approximately equal to the film modulus G_f^* obtained with a second set of disk's and using equations (12) and (14), one can write:

$$\frac{\pi}{4} m \sigma_0 \frac{h_c}{b} \left(\frac{m'}{m' - m} \right) = \frac{\pi}{4} m^* \sigma_0^* \frac{h_c^*}{b^*} \left(\frac{m'^*}{m'^* - m^*} \right) \tag{15}$$

where * denotes variables from the second set of experiments.

Simplifying equation (15) and noting that the contact pressure σ_0 is the same for both sets of tests yields

$$\frac{m^*}{m} = \left[\frac{m}{m'^*} + \frac{h_c^*}{h_c} \frac{b}{b^*} \left(1 - \frac{m}{m'} \right) \right]^{-1} \tag{16}$$

The slope of two elastic bodies in dry rolling traction contact m' can be deduced from reference 25 as follows: The creep in the x-direction, $\Delta U/U$, and that in the

y-direction, $\Delta V/V$, are shown in reference 25 to be related to the surface traction forces F_x and F_y by

$$\left(\frac{\Delta U}{U}\right) = \frac{1}{A_{11}} \frac{F_x}{abG_s} \tag{17}$$

$$\left(\frac{\Delta V}{V}\right) = \frac{1}{A_{22}} \frac{F_7}{abG_s} \tag{18}$$

where A_{11}, A_{22} are Kalker coefficients in x and y direction, respectively, given in reference 25 as function of Poisson's ratio, ν, and ellipticity ratio, k (plotted in fig. 7 for $\nu = 0.3$) and where G_s is the shear modulus of the disk material such that, for steel,

$$G_s = \frac{G}{2(1+\nu)} = 79.3 \text{ GPa } (11.5 \times 10^6 \text{ psi})$$

Since

$$m'_x = \frac{F_x/N}{\Delta U/U} \tag{19}$$

$$m'_y = \frac{F_y/N}{\Delta V/V} \tag{20}$$

and

$$\sigma_0 = \frac{3}{2\pi} \frac{N}{ab} \tag{21}$$

then from equations (17) to (21)

$$m'_x = \frac{3}{2\pi} A_{11} \frac{G_s}{\sigma_0} \tag{22}$$

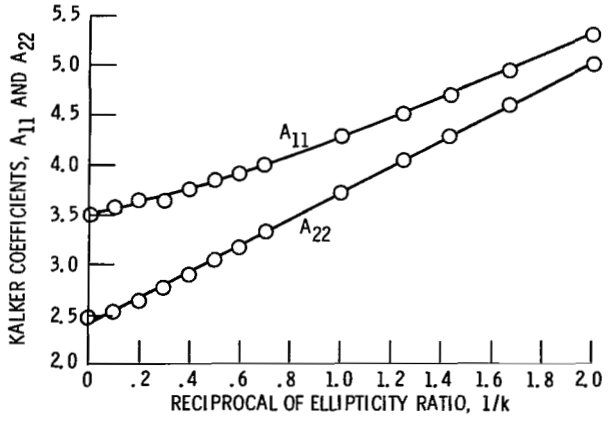

Figure 7. - Kalker coefficients versus reciprocal ellipticity ratio. Poisson's ratio, 0.3. (From ref. 20.)

$$m'_y = \frac{3}{2\pi} A_{22} \frac{G_s}{\sigma_0} \tag{23}$$

If, in equation (16), the variables with asterisks denote the conditions for the case being analyzed by the user and if those without asterisks denote the conditions under which the slope data were generated as obtained from the regression analysis herein, then equations (22) and (23) can be substituted into equation (16). Since the slope data were generated on a sideslip type traction tester (ref. 21), so $m' = m'_y$, and since the slope data will usually be required in the rolling direction, so that $m'^* = m'_x$, equation (16) can be rewritten as

$$\frac{m^*}{m} = \left[\frac{h_c^*}{h_c}\frac{b}{b^*} + \frac{2\pi}{3A_{11}}\frac{\sigma_0}{G_s} m\left(1 - \frac{A_{11}}{A_{22}}\frac{h_c^*}{h_c}\frac{b}{b^*}\right)\right]^{-1} \tag{24}$$

From equations (A7) and (A12) given in the appendix, it is shown that

$$\frac{b^*}{b} = \frac{R_x^*}{R_x}$$

and

$$\frac{h_c^*}{h_c} = \left(\frac{R_x^*}{R_x}\right)^{0.33}$$

Therefore, equation (24) can be simplified further to

$$\frac{m^*}{m} = \left\{\left(\frac{R_x}{R_x^*}\right)^{0.67} + \frac{2\pi}{3A_{11}}\frac{\sigma_0}{G_s} m \times \left[1 - \frac{A_{11}}{A_{22}}\left(\frac{R_x}{R_x^*}\right)^{0.67}\right]\right\}^{-1} \tag{25}$$

For a Poisson's ratio of 0.3, the terms $1/A_{11}$ and A_{11}/A_{22} in equation (25) can be fitted to a good approximation by the following expressions:

$$\frac{1}{A_{11}} = 0.29\, e^{-0.21/k} \tag{26}$$

$$\frac{A_{11}}{A_{22}} = 1.43 - \frac{0.383}{k} + \frac{0.0995}{k^2} \tag{27}$$

(See figs. 8 and 9.) Thus, for the steel test rollers used in reference 18, where $G_s = 79.31$ GPa, equation (25) can be simplified using the approximation shown in equation (26) as follows:

$$\frac{m^*}{m} = \left\{\left(\frac{R_x}{R_x^*}\right)^{0.67} + 7.66 \times 10^{-3}\, m\sigma_0 e^{-0.21/k}\right.$$

$$\times \left[1 - \frac{A_{11}}{A_{22}} \left(\frac{R_x}{R_x^*}\right)^{0.67}\right]\Bigg\}^{-1} \qquad (28)$$

Application of Slope Correction

The slope data presented here were generated with disks having an equivalent radius R_x of 22.57 mm for the Santotrac 50 data and 12.50 mm for TDF-88 data. If the disks to be analyzed have an R_x different than those values, then equation (28) may be solved to determine the appropriate correction factor m^*/m, which can then be applied to the m value calculated from the correlation equation (11) to obtain the corrected slope for the case in question. Alternatively, the m^*/m factor can be found from figure 10 for each of the two test fluids by knowing R_x^*, the ellipticity ratio k, and the contact factor, $m\sigma_0 e^{-0.21/k}$.

It is apparent from figure 10 that, at a given operating condition (i.e., at a given pressure, surface speed, and temperature), m^*/m, and hence slope, increases with disk size. This is because m at constant G is proportional to b/h_c (see eq. (12)) and b/h_c, in turn, is proportional to the 0.67th power of size as shown in the appendix. Increasing σ_0, and thus the second term in equation (25), causes a reduction in m^*/m because at high pressures, nearly all of the compliance is due to the disks whose compliances are size independent. The ellipticity ratio k has a relatively small effect, altering only slightly the Kalker coefficient term in equation (28).

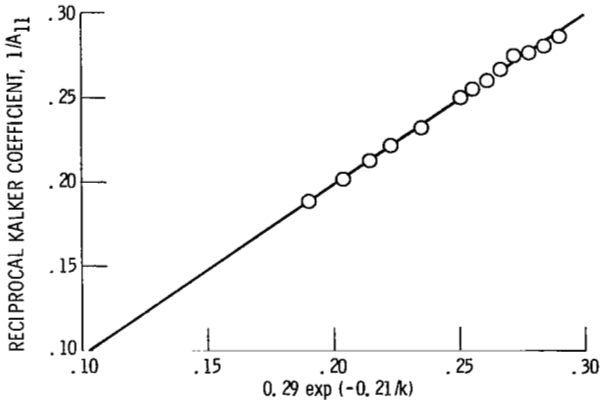

Figure 8. - Comparison of reciprocal Kalker coefficient and its approximation [0.29 exp (-0.21/k)]. Poisson's ratio, 0.3.

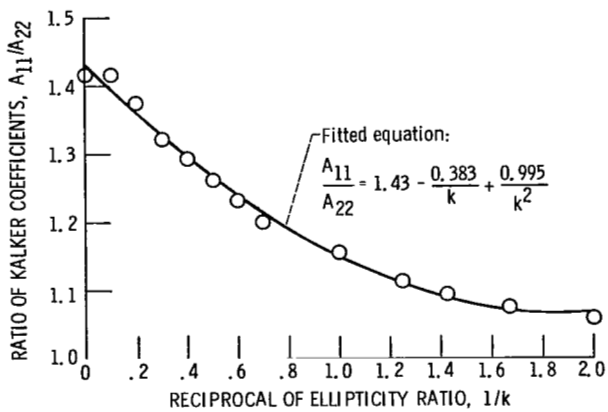

Figure 9. - Ratio of Kalker coefficients versus reciprocal of ellipticity ratio. Poisson's ratio, 0.3.

Results and Discussion

Effect of Operating Conditions

As mentioned before, knowledge of μ and m and the effects that operating conditions have on them is of great importance in the optimization of a traction mechanism. The correlation equations (10) and (11) can be

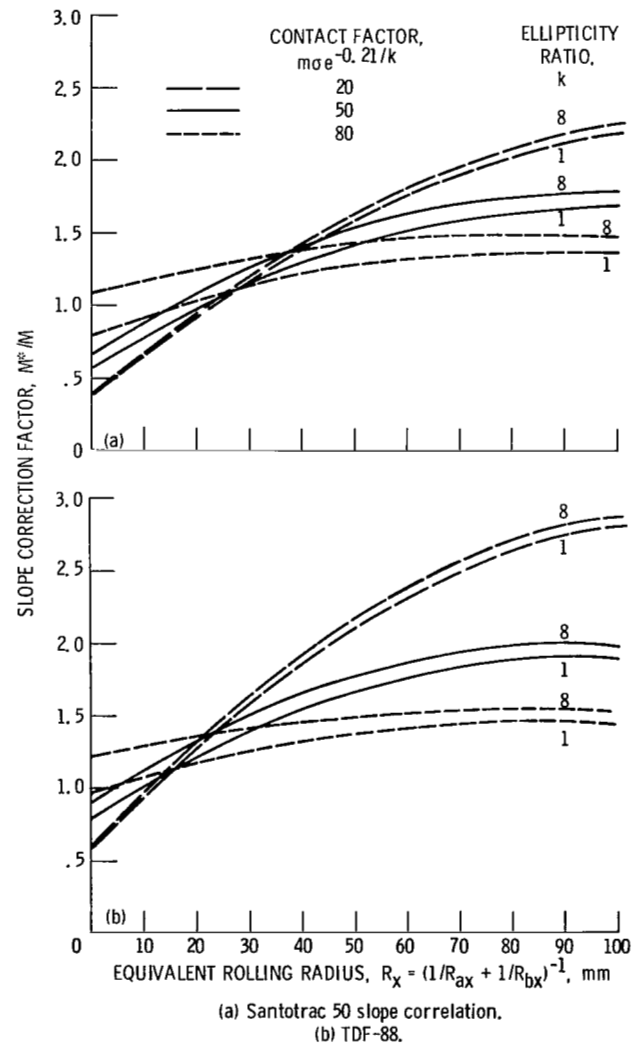

(a) Santotrac 50 slope correlation.
(b) TDF-88.

Figure 10. - Correlation of size effects using slope correction factor.

conveniently used to study the effects that speed, pressure, spin, and lubricant type have on these traction performance factors.

Regression limits. – Based on a limited extrapolation of the test data's operating variables, the likely usable range of the regression equations (10) and (11) is

$\sigma_0 = 1.0$ to 2.5 GPa

$U = 1.0$ to 10 m/s

$T = 30$ to 100 C

$k = 0.5$ to 8

$$\frac{\omega_s \sqrt{ab}}{U} = 0 \text{ to } 0.04$$

Effect of speed and pressure. – As shown in figures 11 to 14, μ and m tend to benefit from an increase in contact pressure or a reduction in surface velocity. Increases in pressure tend to increase the film's resistance to shear, that is, its viscosity and/or "yield" shear strength. However, as suggested by figure 12, the film's shear strength seems to reach some limiting value at some pressure, beyond which there is little or no gain. This behavior has been observed by others (refs. 16 and 26).

Increases in surface velocity are detrimental to μ and m. The loss in traction is due to the increase in lubricant film thickness, which varies approximately with surface velocity to 0.7th power. As shown in the thermal analysis of references 26 to 18, thick films hinder the heat transfer from the center plane of the film to the cooler disk surface, thereby raising the center plane film temperature. As with most materials, increases in temperature tend to reduce the shear strength of the film and thus reduce its effective traction coefficient. The traction coefficient and slope correlated data in figures 11 and 12 tend to reach some minimum value with increasing speed. This is consistent with the observation that film thickness tends to reach some maximum limiting value with increasing speed due to thermal and starvation effects. Figure 12 shows that the slope tends to rise with pressure, reaches a maximum (near 1.5 GPa), and then diminishes as disk compliance becomes significant.

Figure 13 shows typical predicted and measured traction coefficient data for the Santotrac 50 fluid at one

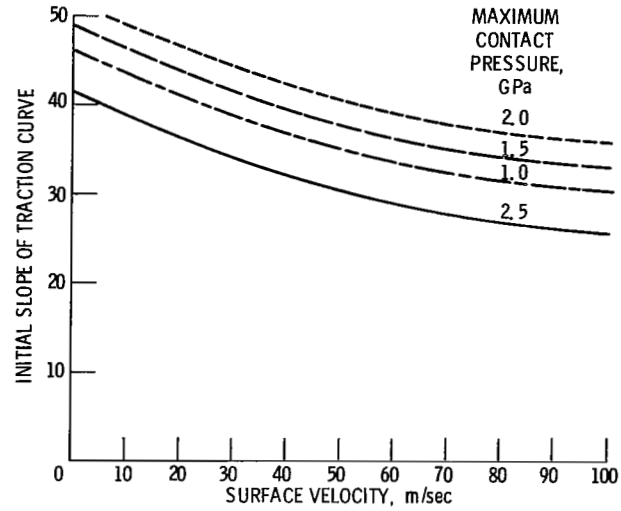

Figure 12. - Effect of surface velocity on initial slope. Predicted from Santotrac 50 correlation. Temperature, 80° C; ellipticity ratio, 5; zero spin.

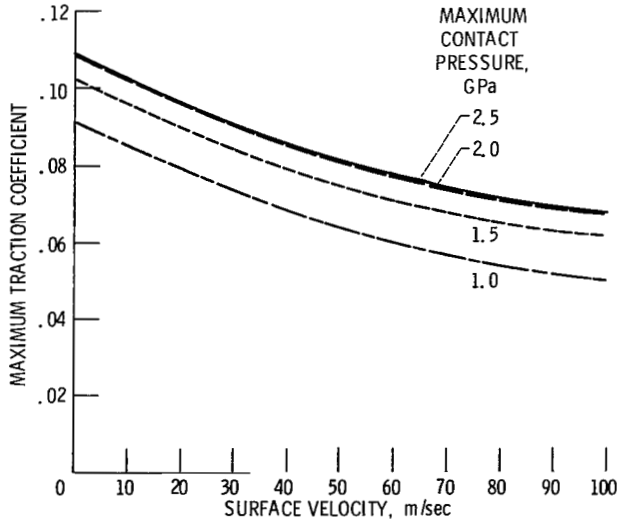

Figure 11. - Effect of surface velocity on maximum traction coefficient. Predicted from Santotrac 50 correlation. Temperature, 80° C; ellipticity ratio, 5; zero spin.

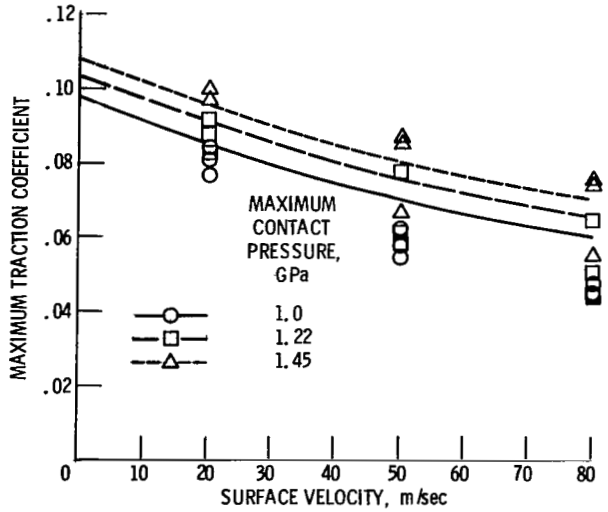

Figure 13. - Comparison of test data and regression analysis. Santotrac 50; temperature, 50° C; zero spin. (Test data from ref. 18.)

operating condition. For this condition the correlation tends to overpredict the traction coefficient at the lowest pressure and two higher speeds, but shows good agreement at the lower speeds and also at higher pressures. The variation in fit exhibited in figure 13 is not uncommon for experimental data of this type, which lacks a high degree of repeatability, as evidenced by the scatter shown for repeat test runs. Taken as a whole, the correlation equations (10) and (11) represent the data well, although there are obviously regions where there is better or worse agreement.

Effect of spin. – Spin, the result of a mismatch in roller radii at contact points on either side of the point of pure rolling has a detrimental effect on traction performance (fig. 14). It occurs in contacts having conical or contoured rolling-elements, such as an angular contact bearing, where the tangent to the point of contact and the axes of rotation are noncoincident. Spin creates a circular slip velocity pattern (fig. 1), which disrupts useful traction; that is, the component of traction in the rolling direction. It also contributes to spin heating, which also reduces the shear strength of the film because of the increased temperatures.

Figure 15 shows that not all lubricants have the same sensitivity to spin. It is apparent that the TDF-88 fluid shows a smaller reduction in μ with nondimensional spin, $\omega_s\sqrt{ab}/U$, than does the Santotrac 50 fluid. At zero-spin the Santotrac 50 fluid shows a small advantage in μ at this operating condition but across the range of operating conditions analyzed, this advantage is not particularly significant. The μ of the Santotrac 50 fluid also shows a somewhat greater sensitivity to maximum contact pressure, but for either fluid there is little incentive in operating above about 2.0 GPa.

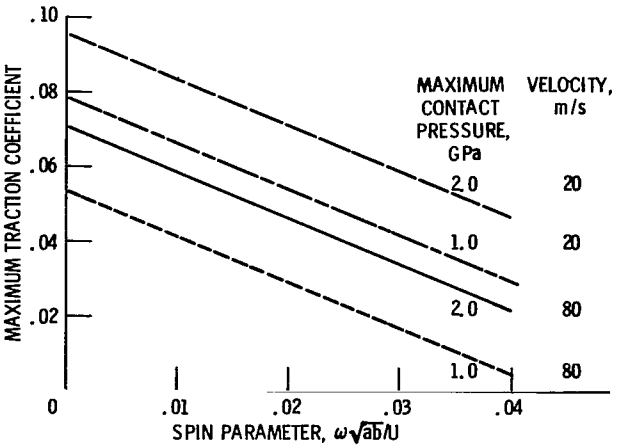

Figure 14. - Effect of spin on maximum traction coefficient from Santotrac 50 correlation. Temperature, 80° C; ellipticity ratio, 5.

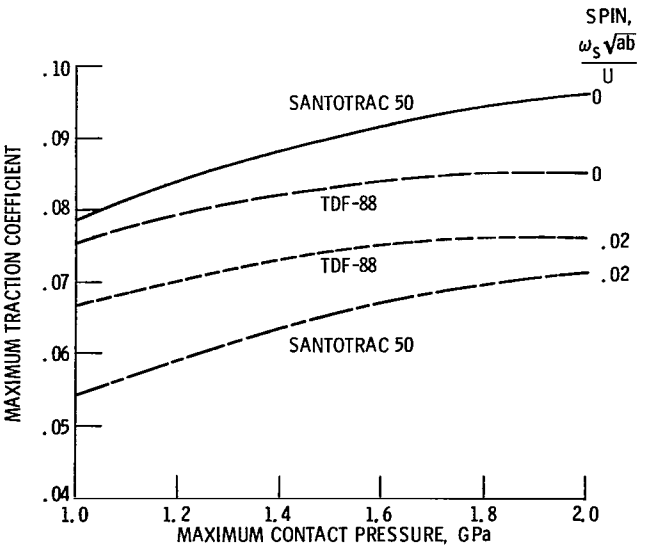

Figure 15. - Effect of spin on maximum traction coefficient. Temperature, 80° C; velocity, 20 m/sec; ellipticity ratio, 5.

Summary of Results

A multivariable regression analysis was performed on traction data for two modern traction fluids, Santotrac 50 and TDF-88, over a wide range of operating conditions. For these test, maximum contact pressure ranged from 1.0 to 1.9 GPa, rolling speeds from 10 to 80 m/sec, oil inlet temperatures from 27° to 73° C, contact ellipse ratios from 1 to 5, and spin angles from 0 to 30°. A total of 187 experimental traction curves for the Santotrac 50 fluid and 147 traction for the TDF-88 fluid were analyzed. An eight-term correlation equation to predict the maximum traction coefficient μ and a six-term equation to predict the initial slope m of the traction curve were developed. Both μ and m must be known at the appropriate operating condition before a traction contact performance analysis, such as the Johnson and Tevaarwerk type, can be conducted. This analysis can be used to determine the traction, creep, spin, torque, and contact power loss associated with a given traction contact. A simplified slope correction method was developed to correct the m correlation for size effect, considering the compliance of the disks themselves. The correlation equations developed were also used to study the effects of different operating conditions on the traction performance of both traction fluids. The following results were obtained.

1. The correlation equations represented the test data satisfactorily. The R-values were better than 0.88 for the traction coefficient correlation and 0.83 for the slope correlation for both traction fluids.

2. Spin caused a significant reduction in maximum traction coefficient for both fluids, but the TDF-88 fluid was less sensitive to spin than the Santotrac 50 fluid.

3. Both traction fluids exhibited comparable, overall traction performance under low spin conditions.

4. Increases in maximum contact pressure benefitted the maximum traction coefficient. At approximately 2.0 GPa the trend reached some upper limit, beyond which there was little or no further gain.

5. Increases in surface velocity were generally detrimental to the maximum traction coefficient. At approximately 100 m/sec, the trend reached some lower limit beyond which there was little or no further reduction.

6. The stiffness of the film-disk combination within the contact as reflected by the slope of the traction curve increased with contact pressure and decreased with speed.

7. At constant operating conditions and ellipticity ratio, an increase in disk size will cause an apparent increase in slope.

Lewis Research Center
National Aeronautics and Space Administration
Cleveland, Ohio, January 21, 1983

Appendix—Effect of Disk Geometry on Relative Contact Size and EHD Film Thickness

The initial slope correction m^*/m given in the main text is to be applied to slope data for the same contact pressure σ_0, rolling speed U, temperature T, ellipticity ratio k, disk material, and lubricant. However, no restrictions are placed on disk size or relative radius of curvatures. The geometry of the disks will affect the size of the contact and relative EHD film thickness as will be shown. In keeping with the main text, the variables with asterisks denote conditions for one set of disks, and those without asterisks referred to another set of data.

Contact ellipse size. – The semimajor and semiminor ellipse diameters are given by

$$a = \epsilon g \tag{A1}$$

$$b = \xi g \tag{A2}$$

where ϵ and ξ are elliptical integrals of first and second kind and are only functions of (R_y/R_x) and where

$$g \propto \left(\frac{N}{\rho}\right)^{1/3} \tag{A3}$$

Since

$$\rho = \frac{1}{R_x} + \frac{1}{R_y} = \frac{1}{R_x}\left(1 + \frac{R_x}{R_y}\right)$$

then

$$b \propto \xi \left(\frac{NR_x}{1 + R_y/R_x}\right)^{1/3} \tag{A4}$$

Since $k = a/b$ and since the normal load is related to σ_0 by

$$N = \frac{2\pi}{3} ab\sigma_0 = \frac{2\pi}{3} b^2 k \sigma_0 \tag{A5}$$

equation (A4) becomes

$$b \propto \xi^3 \left[\frac{k\sigma_0 R_x}{1 + (R_x/R_y)}\right] \tag{A6}$$

For two experiments having equal σ_0 and k, that is, $\sigma_0^* = \sigma_0$ and $k^* = k$,

$$\epsilon^* = \epsilon \qquad \xi^* = \xi \qquad \left(\frac{R_x}{R_y}\right)^* = \frac{R_x}{R_y}$$

The relative contact ellipse diameters from equation (A6) thus become

$$\frac{b^*}{b} = \frac{R^*_x}{R_x} \tag{A7}$$

Therefore, the relative contact ellipse diameters between the two sets of tests are only a function of the relative equivalent radii of curvature in the rolling direction R_x, defined as

$$\frac{1}{R_x} = \frac{1}{r_{Ax}} + \frac{1}{r_{Bx}} \tag{A8}$$

where r_{Ax} and r_{Bx} are the principal rolling radii of bodies A and B, respectively.

Film thickness. – In reference 29 the central EHD film thickness is given as

$$\frac{h_c}{R_x} = 2.69\left(\frac{\eta_0 U}{E' R_x}\right)^{0.67} (\alpha E')^{0.53} \times \left(\frac{N}{E' R_x^2}\right)^{-0.067} (1 - e^{-0.73k}) \tag{A9}$$

For two experiments under the same operating conditions with the same lubricant and disk material, the relative film thickness h_c^*/h_c can be written as

$$\frac{h_c^*}{h_c} = \left(\frac{R_x^*}{R_x}\right)\left(\frac{R_x}{R_x^*}\right)^{0.67}\left(\frac{N^*}{N}\right)^{-0.067}\left(\frac{R_x}{R_x^*}\right)^{-0.134} \tag{A10}$$

From equations (A5) and (A7)

$$\frac{N^*}{N} = \left(\frac{b^*}{b}\right)^2 = \left(\frac{R_x^*}{R_x}\right)^2 \tag{A11}$$

Substituting equation (A11) into equation (A10) and simplifying yields:

$$\frac{h_c^*}{h_c} = \left(\frac{R_x^*}{R_x}\right)^{0.330} \tag{A12}$$

References

1. Rohn, D.A.; Loewenthal, S.H.; and Coy, J.J.: Sizing Criteria for Traction Drives. NASA CP-2210, 1982.
2. Wernitz, W.: Friction at Hertzian Contact with Combined Roll and Twist. Rolling Contact Phenomena, J.B. Bidwell, ed., Elsevier Publishing Co., 1962, pp. 132-156.
3. Magi, M.: On Efficiencies of Mechanical Coplanar Shaft Power Transmissions. Chalmers University, Gothenburg, Sweden, 1974.
4. Poon, S.Y.: Some Calculations to Assess the Effect of Spin on the Tractive Capacity of Rolling Contact Drives. Proc. Inst. Mech. Eng. (London), vol. 185, no. 76/71, 1970, pp. 1015-1022.
5. Lingard, S.: Tractions at the Spinning Point Contacts of a Variable Ratio Friction Drive. Tribol. Int., vol. 7, no. 5, Oct. 1974, pp. 228-234.
6. Daniels, B.K.: Traction Contact Optimization. ASLE Preprint 79-LC-1A-1, 1979.
7. Johnson, K.L.; and Tevaarwerk, J.L.: Shear Behavior of Elastohydrodynamic Oil Films. Proc. R. Soc. (London), Ser. A., vol. 356, no. 1685, Aug. 1977, pp. 215-236.
8. Clark, O.H.; Woods, W.W.; and White, J.R.: Lubrication at Extreme Pressures with Mineral Oil Films. J. Appl. Phys., vol. 22, no. 4, Apr. 1951, pp. 474-483.
9. Smith, F.W.: The Effect of Temperature in Concentrated Contact Lubrication. ASLE Trans., vol. 5, no. 1, Apr. 1962, pp. 142-148.
10. Johnson, K.L.; and Cameron, R.: Shear Behavior of Elastohydrodynamic Oil Films at High Rolling Contact Pressures. Proc. Inst. Mech. Eng., London, vol. 182, pt. 1, no. 14, 1967, pp. 307-319.
11. Tevaarwerk, J.L.: Traction Drive Performance Prediction for the Johnson and Tevaarwerk Traction Model. NASA TP-1530, Oct. 1979.
12. Tevaarwerk, J.L.; and Johnson, K.L.: The Influence of Fluid Rheology on the Performance of Traction Drives. J. Lubr. Technol., vol. 101, no. 3, July 1979, pp. 266-274.
13. Bair, S.; and Winer, W.O.: Some Observation in High Pressure Rheology of Lubricants. J. Lubr. Technol., vol. 104, No. 3, July 1982, pp. 357-364.
14. Walowit, J.A.; and Smith, R.O.: Traction Characteristics of a MIL-L-7808 Oil. ASME Paper 76-Lubs-19, May 1976.
15. Hewko, L.O.; Rounds, F.G., Jr.; and Scott, R.L.: Tractive Capacity and Efficiency of Rolling Contacts. Rolling Contact Phenomena, J.B. Bidwell, ed., Elsevier Publishing Co., 1962, pp. 157-185.
16. Gaggermeier, H.: Investigations of Tractive Force Transmission in Variable Traction Drives in the area of Elastohydrodynamic Lubrication, Ph.D. Dissertation, Technical University of Munich, July 1977.
17. Gupta, P.K.; et al.: On the Traction Behavior of Several Lubricants. J. Lubr. Technol., vol. 103, no. 1, Jan. 1981, pp. 55-64.
18. Tevaarwerk, J.L.: Traction Contact Performance Evaluation at High Speeds. DOE/NASA/0035-1, NASA CR-165226, 1981.
19. Cheng, H.S.; and Sternlicht, B.: A Numerical Solution for the Pressure, Temperature, and Film Thickness Between Two Infinitely Long Lubricated Rolling and Sliding Cylinders under Heavy Loads. J. Basic Eng., vol. 87, no. 3, Sept. 1965, pp. 695-707.
20. Dowson, D.; and Whitaker, B.A.: A Numerical Procedure for the Solution of Elastohydrodynamic Problem of Rolling and Sliding Contacts Lubricated by a Newtonian Fluid. Proc. Inst. of Mech. Eng., London, vol. 180, pt. 3B, 1966, pp. 57-71.
21. Kannel, J.W.; and Walowit, J.A.: Simplified Analysis for Tractions Between Rolling-Sliding Elastohydrodynamic Contacts. J. Lubr. Technol., vol. 93, no. 1, Jan. 1971, pp. 39-46.
22. Draper, N.R.; and Smith, H.: Applied Regression Analysis. Second ed. John Wiley & Sons, Inc., 1981.
23. Johnson, K.L.; and Roberts, A.D.: Observations of Viscoelastic Behaviour of an Elastohydrodynamic Lubricant Film. Proc. R. Soc. (London), Ser. A., vol. 337, no. 1609, Mar. 1974, pp. 217-242.
24. Johnson, K.L.; Nayak, L.; and Moore, A.J.: Determination of Elastic Shear Modulus of Lubricants from Disc Machine Tests. Elastohydrodynamics and Related Topics, D. Dowson, ed., Mechanical Engineering Publications for the Institute of Tribology, 1979, pp. 204-213.
25. Kalker, J.J.: On the Rolling Contact of Two Elastic Bodies in the Presence of Dry Friction. Ph.D. Dissertation, Rept. No. WTHD-52, Technische Hogeschool, Delft, Netherlands, 1973.
26. Johnson, K.L.; and Greenwood, J.A.: Thermal Analysis of an Eyring Fluid in Elastohydrodynamic Traction. Wear, vol. 61, 1980, pp. 353-374.
27. Tevaarwerk, J.L.: Traction Calculations Using the Shear Plane Hypothesis. Thermal Effects in Tribology, D. Dowson, ed., Mechanical Engineering Publications for the Institute of Tribology, 1980, pp. 201-213.
28. Tevaarwerk, J.L.: Thermal Influence on the Traction Behavior of an Elastic/Plastic Model. Friction and Traction. D. Dowson, et al., eds., Westbury House, 1981, pp. 302-319.
29. Hamrock, B.J.; and Dowson, D.: Isothermal Elastohydrodynamic Lubrication of Point Contacts, Part III—Fully Flooded Results. J. Lubr. Technol., vol. 99, No. 2, Apr. 1977, pp. 264-276.

1. Report No.	2. Government Accession No.	3. Recipient's Catalog No.
NASA TP-2154		

4. Title and Subtitle	5. Report Date
REGRESSION ANALYSIS OF TRACTION CHARACTERISTICS OF TWO TRACTION FLUIDS	May 1983
	6. Performing Organization Code 505-32-42

7. Author(s)	8. Performing Organization Report No.
Stuart H. Loewenthal and Douglas A. Rohn	E-1300
	10. Work Unit No.

9. Performing Organization Name and Address	11. Contract or Grant No.
National Aeronautics and Space Administration Lewis Research Center Cleveland, Ohio 44135	
	13. Type of Report and Period Covered
12. Sponsoring Agency Name and Address	Technical Paper
National Aeronautics and Space Administration Washington, D. C. 20546	14. Sponsoring Agency Code

15. Supplementary Notes

16. Abstract

A multivariable regression analysis was performed on traction data for two modern traction fluids, Santotrac 50 and TDF-88, over a wide range of operating conditions. For these tests maximum contact pressures ranged from 1.0 to 1.9 GPa; rolling speeds from 10 to 80 m/sec; oil inlet temperature from 27° to 73° C; contact ellipse ratios from 1 to 5; and spin angles from 0 to 30°. A total of 187 experimental traction curves for the Santotrac 50 and 147 traction curves for the TDF-88 fluid were analyzed. An eight-term correlation equation to predict the maximum traction coefficient μ, and a six-term correlation equation to predict the initial slope m of the traction curve were developed. Both μ and m must be known at the appropriate operating condition before a traction contact performance analysis, such as the Johnson and Tevaarwerk type, can be conducted. A performance analysis can be used to determine the traction, creep, spin torque, and contact power loss associated with a given traction contact. A simplified slope correction was developed to correct the slope correlation for size effect considering the compliance of the disks. The correlation equations developed were also used to study the effects of different operating conditions on the traction performance of each traction fluid. The correlation equations were found to fit the data reasonably well over the range of operating conditions. Both traction fluids exhibited a loss in traction with increases in spin, but the losses with the TDF-88 fluid were not as severe as those with Santotrac 50. Overall, both fluids exhibited similar performance, showing an increase in traction with contact pressure up to about 2.0 GPa, and a reduction in traction with higher surface speeds up to about 100 m/sec. The apparent stiffness of the traction contact, that is, film-disk combination, increases with contact pressure and decreases with speed.

17. Key Words (Suggested by Author(s))	18. Distribution Statement
Traction; Traction fluids; Traction lubricants; Traction drives; Traction transmission; Lubricants	Unclassified - unlimited STAR Category 37

19. Security Classif. (of this report)	20. Security Classif. (of this page)	21. No. of Pages	22. Price*
Unclassified	Unclassified	16	A01

* For sale by the National Technical Information Service, Springfield, Virginia 22161

NASA-Langley, 1983

2 1 1U,D, 830512 S00903DS
DEPT OF THE AIR FORCE
AF WEAPONS LABORATORY
ATTN: TECHNICAL LIBRARY (SUL)
KIRTLAND AFB NM 87117